Amplifying the Signal of Metal Oxide Gas Sensors for Low Concentration Gas Detection

Xinyuan Zhou, Ying Wang, Jinxiao Wang, Zheng Xie, Xiaofeng Wu, Ning Han, and Yunfa Chen

***Abstract*— Nowadays, detection of trace concentration gases is still challenging for portable sensors, especially for the low-cost and easily operated metal–oxide–semiconductor (MOX) gas sensors. In this paper, a widely applicable amplification circuit is designed and fabricated to evidently enhance the signal of the MOX sensors by adding a field effect transistor (FET) into the conventional circuits. By optimizing the FET parameters and the loading resistance, this amplification circuit enables the commercial Figaro TGS2602 toluene sensors response effectively to the highest permissive limit (0.26 ppm) of toluene in indoor air of cars, with the detection limit of ∼0.1 ppm. Furthermore, this circuit can also make the commercial Hanwei MP502 acetone sensors and MQ3 ethanol sensors response to the 1–2-ppm acetone in breath of diabetes and 2-ppm ethanol for fast and effectively drinker driver screening. The mechanism is investigated to be the gate voltage induced resistance change of the FET, with the highest theoretically estimated and experimentally measured magnification factor of 5–6. This FET amplifier can effectively enable the ppm level commercial MOX sensors response to sub-ppm level gases, promising for MOX gas sensor integration and also for other kind of resistive sensors.**

***Index Terms*— Environment and health, field effect transistor, amplifier, low concentration, metal oxide semiconductor sensor**

I. Introduction

DUE TO the easy fabrication, facile operation and relatively high sensitivity, metal oxide semiconductor (MOX) gas sensors have been widely adopted as inflammable and explosive gas alarms, which are working for gases at relatively high concentration of percent per million (ppm) to percentage levels. In recent years, people are aiming at detecting the low concentration gases at sub-ppm levels for health, environment and so on [1]–[6]. For example, many countries all over the world recommend the highest permissive concentration of volatile organic compounds (VOCs) should be in the sub-ppm level in cars. For example toluene should be less than 1.0 mg/m^3 (∼0.26 ppm) because it is stimulus to the skin, eyes, and respiratory system even at low concentrations (e.g. Vehicle Interior Air Quality, VIAQ and Chinese guideline GB/T 27630-2011). On the other side, disease analyses show that the diabetes would exhale acetone with criteria of 1-2 ppm because of the disability of metabolism, and drinker drivers will exhale ethanol of several to hundreds of ppm in their breath [7]–[9]. In these cases, the MOX sensors should have higher sensitivity, i.e. lower detection limit at ppb-ppm level, in order to response effectively to those typical trace content gases. However, except for some laboratory results, it is still a challenge for commercial MOX sensors to have such low detection limit, and thus many researches are focused on improving the gas response of MOX sensors.

The general method is to improve the gas response of MOX sensing materials such as SnO_2, In_2O_3, ZnO, etc., by ways such as doping with other elements [8], [10]–[12], surface functionalization [13]–[17], heterojunction [18]–[20], core/shell structure [21]–[23], Micro-Electro-Mechanical System fabrication [24], [25], and so on. For example, Guan et al. found that the Zn doped SnO_2 had 3.2 times higher response (resistance ratio Ra/Rg of the sensor resistance in air Ra and in gas Rg) to ethanol (14.4 to 100 ppm) compared with the pure SnO_2 [10]. Zou *et al.* found that Au, Ag, and Pt surface functionalization would not only enhance the gas response of In_2O_3 nanowire sensors, but also increase the selectivity to CO, ethanol and H_2 [15]. And toluene gas sensing performance is also greatly improved by rational material design such as SnO_2/SnO_2 yolk-shell structures (28.6 to 20 ppm) reported by Bing *et al.* [26], rGO/Co_3O_4 composites (11.3 to 5 ppm) by Bai *et al.* [27], Pt decorated SnO_2-ZnO core-shell structure (279 to 0.1 ppm) by Kim *et al.* [22]. Though these researches pushed the MOX gas sensors to step forwards greatly, there are still limited commercial sensors with acceptable responses to the trace content gases. For example, commercial toluene gas sensors (TGS2602, Figaro, Japan) have detection limit of ∼1 ppm with response of ∼ 3, which cannot yet effectively response to the toluene at concentrations of ∼ 0.26 ppm recommended by VIAQ.

Though the sensor signal can also be enhanced by external integrated circuits using operational amplifier, special care should be taken to the offset adjustment and noise filtering etc. [28]-[31], and the complicated circuit design would degenerate the low-cost advantage of the MOX sensors. In this study, a widely applicable sensor signal amplification method is developed by adding a field effect transistor (FET) to increase the responses of MOX sensors and thus lower the detection

Manuscript received December 8, 2016; revised February 6, 2017 and March 2, 2017; accepted March 3, 2017. Date of publication March 7, 2017; date of current version April 10, 2017. This work was supported in part by the National Key Research and Development Program under Grant 2016YFC0207101, in part by the National Natural Science Foundation of China under Grant 51272253, in part by the Guangdong Innovative and Entrepreneurial Research Team Program under Grant 2014ZT05C146, and in part by the State Key Laboratory of Multiphase Complex Systems under Grant MPCS-2014-C-01. The associate editor coordinating the review of this paper and approving it for publication was Dr. Camilla Baratto.

The authors are with the State Key Laboratory of Multiphase Complex Systems, Institute of Process Engineering, Chinese Academy of Sciences, Beijing 100190, China, also with the University of Chinese Academy of Sciences, Beijing 10049, China, and also with the Center for Excellence in Regional Atmospheric Environment, Institute of Urban Environment, Chinese Academy of Sciences, Xiamen 361021, China (e-mail: zhouxinyuan14@mails.ucas.ac.cn; nhan@ipe.ac.cn;chenyf@ipe.ac.cn).

This paper has supplementary downloadable multimedia material available at http://ieeexplore.ieee.org provided by the authors. The Supplementary Material contains Figs. S1 and S2. This material is 206 KB in size.

Digital Object Identifier 10.1109/JSEN.2017.2678985

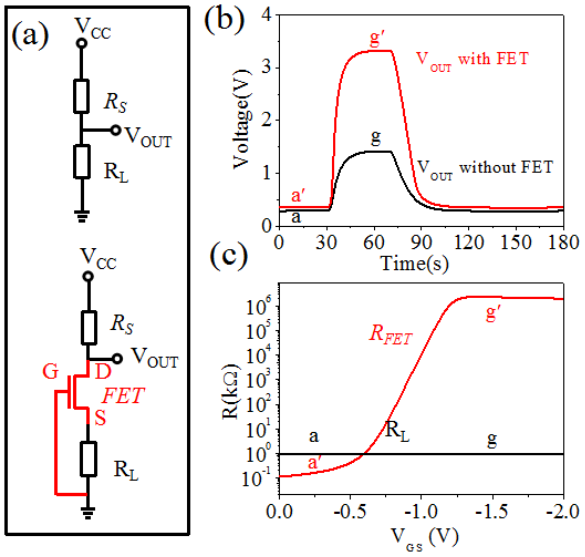

Fig. 1. Principle of the designed amplification circuit: (a) comparison of the conventional and the designed amplification electric circuit of gas sensors by adding FET; (b) the voltage output comparison. Points a and a' are baseline voltage in air, and g and g' are response voltage in detectants without and with FET; (c) the resistance change of FET with its gate voltage. In air, R_{FET} is small at a' point compared with R_L at a point. But R_{FET} increases a lot in detectants at point g' as compared with the fixed resistance of R_L at point g. The increased R_{FET} is the main principle of the voltage amplification circuit.

limits. To show the effect and make the technology more general, commercial toluene sensors (Figaro TGS2602, Japan), acetone sensors (Hanwei MP502, China) and ethanol sensors (Hanwei MQ3, China) are adopted as the examples with signal amplified by the commercial FETs (K series, Japan). The amplification method decreases the detection limit of TG2602, MP502 and MQ3 to ~0.1 ppm toluene, <2 ppm acetone and <2 ppm ethanol, which can be readily used for large scale integration into portable alarms. It should be noted that this response amplification method can also be applied to other kind of resistance sensors, showing the promise of this technology for MOX gas sensors for detection of trace concentration gases and also for other resistive sensors to effectively amplify the signal.

II. Principle of the Amplification Circuit

Taking n-type MOX sensor in detection of reductive gases for an example, the MOX gas sensor (R_S) is traditionally working with a tandem connection to a load resistor (R_L) as shown in Fig. 1a. After a voltage (Vcc) is biased, the partial voltage of the R_L is taken as the sensor signal (V_{OUT}). The R_L is normally well chosen so that V_{OUT} in air is low behaving as the baseline. When the sensor gets in contact with detectants such as toluene, the sensor resistance R_S will decrease, resulting in increase of V_{OUT} and thus generating a voltage signal as shown in Fig. 1b. It is obvious that the signal is merely produced by the R_S change.

In our proposed circuits in Fig. 1a, an n-type FET (red color) is connected with R_L and R_S with source (S) and drain (D) electrodes. The gate electrode (G) is then connected to the lower potential side of R_L generating a minus gate voltage for the FET. The value of R_L is well chosen so as to make the FET work at ON state in air (e.g. $10^2\Omega$ at point a' in Fig. 1c). Similar to the traditional circuits, V_{OUT} will also increase when the sensor contacts reductive gases, and so does the absolute gate to source voltage (V_{GS}) of the FET. At the same time, the increased $|V_{GS}|$ drives the FET to OFF state (qualitatively being point g' in Fig. 1c, 10^9 Ω), meaning its resistance will increase sharply. The increased FET resistance gives feedback to the circuit again to enhance the V_{OUT}, which finally equilibrates to a maximum far higher than that without the FET. It should be noted that this FET signal amplification is in distinguishingly distinct with conventional operational amplifiers which is aiming at enhancing the V_{OUT} in traditional circuits.

Quantitatively, the conventional output voltage V_{OUT} can be calculated as:

$$V_{OUT} = V_{CC}R_L/(R_L + R_S) = V_{CC}/(1 + R_S/R_L). \quad (1)$$

where it is clear that V_{OUT} will increase with decrease of R_S when contacting detectants. Similarly, in the proposed amplification circuit, V_{OUT} can be written as:

$$V_{OUT} = V_{CC}/[1 + R_S/(R_L + R_{FET})]. \quad (2)$$

It is therefore, V_{OUT} will be enhanced greatly if R_{FET} increase together with the R_S decrease, meaning amplifying the voltage output.

From (1), it is easy to derive the conventional response of MOX sensors as:

$$R_{S,a}/R_{s,g} = (V_{CC}/V_{OUT,a} - 1)/(V_{CC}/V_{OUT,g} - 1). \quad (3)$$

where $V_{OUT,a}$ and $V_{OUT,g}$ are the output voltage of the conventional circuit in Fig. 1a. The apparent response of the FET circuit is also calculated in the same way, as derived from (2):

$$R_{S,a}/R_{s,g} \times (R_L + R_{FET,g})/(R_L + R_{FET,a}) = (V_{CC}/V_{OUT,a} - 1)/(V_{CC}/V_{OUT,g} - 1). \quad (4)$$

Therefore, the magnification factor (MF) can be easily derived by (3) and (4) to be $(R_L+R_{FET,g})$ / $(R_L + R_{FET,a})$, i.e. resistance change of the load $(R_L+ R_{FET})$, which will be discussed in detail in the discussion.

III. Experimental

Commercial gas sensors are bought from the market, which are toluene sensor (Figaro TGS2602, Japan), ethanol sensor (Hanwei MQ3, China) and acetone sensor (Hanwei MP502, China). Commercial FETs are also bought from the market, which are K168, K514 and K544 (Sanyo, Japan). All the electronic devices are used without any modification. The gas sensing property is measured using static measurement system designed for sensor products (Hanwei WS-30A, China) as details reported in the literature [7], [10], [27], [32]. Load resistance card is the standard accessary of the system, and the FET is soldered onto the resistance card with D, S, and G electrodes shown in Fig. 1a. Toluene, ethanol and acetone gases with difference concentrations (> 1 ppm) are generated by dropping certain amounts of the liquid with a micro syringe onto an evaporator in the test chamber (total volume 18 L).

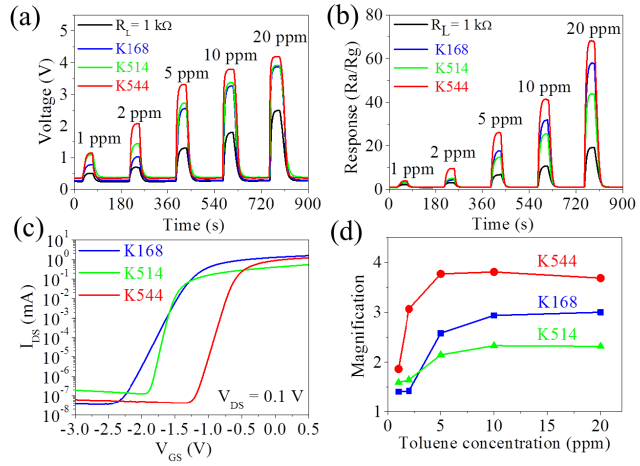

Fig. 2. Response comparison of toluene sensor with and without FET. (a) output voltage of the toluene sensor with R_L = 1.0 kΩ with and without FETs, (b) response of the toluene sensor calculated from (a), (c) I_{DS}-V_{GS} curves of the FETs K168, K514 and K544, and (d) magnification of the amplification circuit with three types of FETs.

Toluene gases with 0.1 and 0.3 ppm are produced by adding certain volume of 50 ppm standard gas into the chamber. Response is defined as the resistance ratio R_{Sa}/R_{Sg} of the sensor resistance (R_S) in air and in detectants in the conventional circuit and was calculated by equation (3). The apparent response of the sensor in FET amplification circuit is calculated by equation (4) assuming a fixed value of R_{FET} at the ON state in air on the baseline. The I-V curves of the FET are measured by Keithley 4200 semiconductor analyzer.

IV. Results and Discussion

A. Toluene Sensor

The toluene sensor TGS2602 is used as a proof of concept of this proposed signal amplification circuit. According to the manual, V_{CC} is 5 V and R_L should be > 0.45 kΩ. The voltage output is shown in Fig. 2a by using R_L = 1.0 kΩ with toluene concentration varying from 1 to 20 ppm. It is clear that all the FET circuits can enhance the voltage output, with the maximized amplification effect of K544. The corresponding response and apparent response are calculated in Fig. 2b. It is noticed that the response to 1 ppm toluene is 2-3, in accordance with that of the manual though there would be device-device variations and gas concentration variations. However, when K544 FET is connected into the circuit as proposed, the response can be enhanced to ~5 showing the amplification effect. From the transfer curves (I_{DS} - V_{GS}) in Fig. 2c, the K544 FET has the largest I_{DS}-V_{GS} slope (the smallest subthreshold swing). The largest slope makes K544 the most sensitive to the gate voltage change, leading to the largest amplification effect. The magnification factor (MF, ratio of apparent response with FET and response without FET) of K544, K168 and K514 are shown in Fig. 2d, where it is clearly shown that K544 works better than the other two FETs. The MFs are 2-4 depending on the gas concentrations, because the varied gas concentrations would generate different gate voltage on the FET and thus make FET work on different resistances.

From the working principle, the V_{GS} of FET is the partial voltage of the resistor load R_L, which should therefore be optimized to get a maximum amplification. In our study, R_L is set as 0.5, 1.0, 2.0, 3.0 and 4.7 kΩ, and the typical response curves with and without FET K544 are shown in Fig. 3a-c and in Fig. S1 in supporting information. It is obvious that output voltages are all enhanced greatly by the FET amplification circuits. The resultant amplifications are shown in Fig. 3d by testing at least 5 sensors, where it is obvious that a maximum MF of ~5 is obtained using the 2.0 kΩ resistor. The optimized circuit is then used to test the response to toluene with lower concentration such as 0.1 and 0.3 ppm as shown in Fig. 3e. A significant voltage response can be seen in the curve with the K544 FET. Otherwise, the voltage change is neglectable to 0.1 and 0.3 ppm toluene in the conventional circuit. The responses are calculated in Fig. 3f, where it is clear that responses of 1.5, 2.5 and 7.2 are obtained to 0.1, 0.3 and 1 ppm toluene, which are much higher than those without FET. VIAQ and many countries recommend a maximum permitted limit of 1.0 mg/m^3 (0.26 ppm) toluene in indoor air of a car, which is emitted by the decorations. Therefore, whether the toluene concentration is above the standard in cars can be easily assessed using the FET amplification circuit with detection limit of ~0.1 ppm. And more importantly, all the electronics can be readily purchased from the market and be integrated easily onto a board.

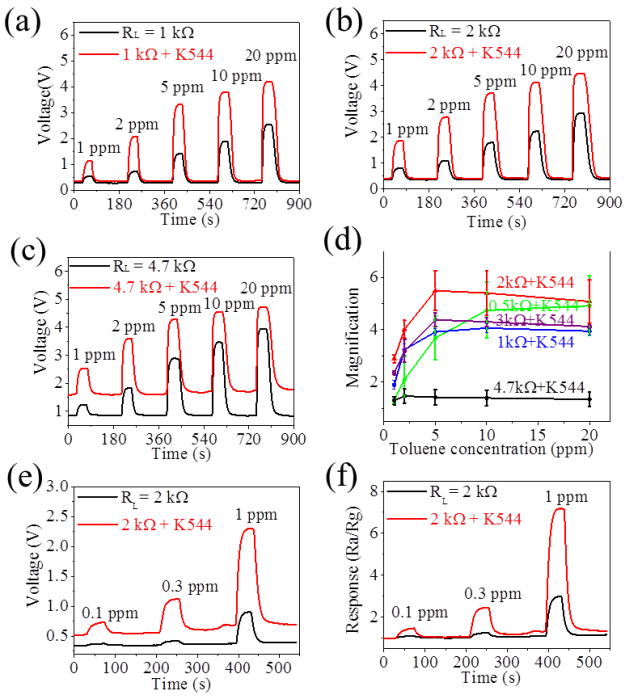

Fig. 3. Amplification effect of toluene sensor using FET K544. Output voltage by connecting resistor of (a) R_L = 1.0 kΩ, (b) R_L = 2.0 kΩ, (c) R_L = 4.7 kΩ, (d) magnification of the response by FET amplification circuit, (e) and (f) comparison of output voltage and response to low concentration toluene using amplification circuit FET K544 connecting 2.0 kΩ resistor.

B. Acetone and Ethanol Sensor

In order to extend the amplification circuit to other MOX sensors, commercial acetone and ethanol sensors are adopted in this study. According to the disease analyses, the diabetes will exhale acetone in the breath with the criteria of 1-2 ppm

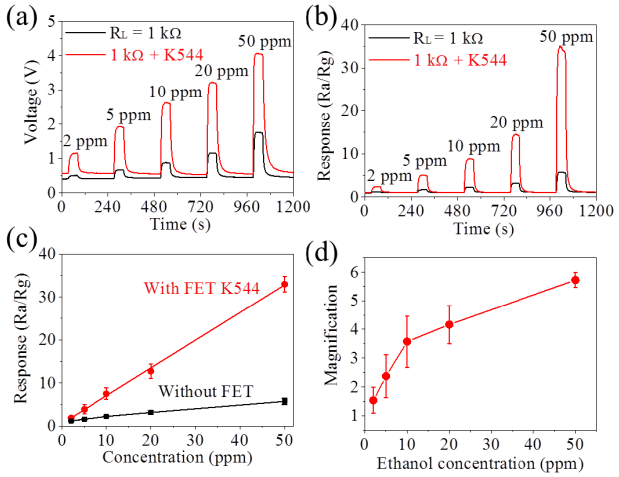

Fig. 4. Signal amplification of acetone sensors: (a) output voltage with and without FET K544, (b) the calculated response curves, (c) the response comparison of the sensor with and without FET, and (d) magnification effect of the acetone sensor at different concentrations by the new electric circuit with FET K544.

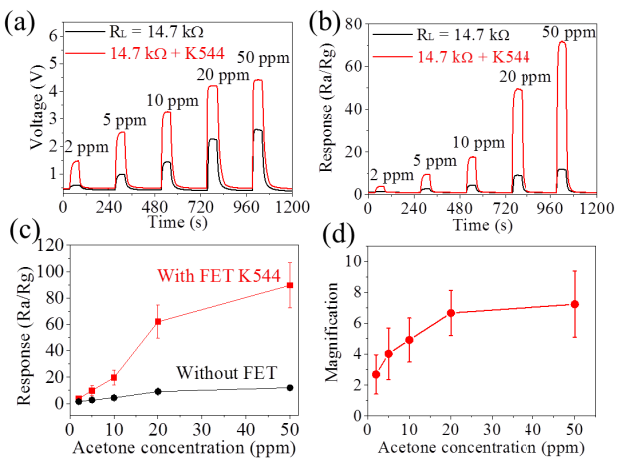

Fig. 5. Signal amplification of ethanol sensors: (a) output voltage with and without FET K544, (b) the calculated response curves from (a), (c) the response comparison of the sensor with and without FET, and (d) magnification effect of the ethanol sensor at different concentrations by the new electric circuit with FET K544.

because of metabolism disability. Therefore, there are many reports on highly sensitively acetone sensing materials, such as In_2O_3, $ZnFe_2O_4$ etc. [7], [33]. However, the commercial MOX acetone sensors (Hanwei MP502) have relatively low response to acetone at such low concentration, e.g. ~0.1 V response to 2 ppm as shown in the response curve in Fig. 4a. On the other side, the response is greatly enhanced using K544 FET amplification circuit, with ~1.0 V voltage response to 2 ppm at the optimized load resistance of 14.7 kΩ in Fig. 4a. Therefore, this amplification circuit enhances the detection limit of the acetone sensor, which is suitable for diabetes analysis by detecting the 1-2 ppm acetone concentration in the breath. The response curve is further calculated in Fig. 4b, where one can clearly see the response to 2 ppm using FET is already similar to that to 10 ppm without FET. The responses are then compared as shown in Fig. 4c, showing a great response enhancement MF, which is 3-6 magnification as calculated in Fig. 4d.

In the meanwhile, the drinkers are prohibited from driving all over the world, and a blood ethanol concentration of 10-80 mg/100 ml is recommended by world health organization and other countries (e.g. Chinese guideline GB 19522-2010). The breath ethanol concentration serves as a fast detection method, with the exhale concentration of ethanol of 20-170 ppm. Commercial ethanol sensor (Hanwei MQ3) can detect ethanol at this concentration as shown in Fig. 5a. However, using the amplification circuit again, the responses are enhanced greatly with the detection limit of < 2 ppm, providing more opportunity for the ethanol detectors to work well on the fast screening of drinker drivers. The responses are calculated in Fig. 5b and c with a MF of 2-6 as shown in Fig. 5d.

Therefore, the FET amplification circuit can effectively enhance the response of MOX sensors, and thus the detection limit is greatly extended to trace concentrations. Though the responses are still lower than some of the laboratory ones as compared in Table I, these commercial sensors with the FET amplification circuits are already ones of the highest responses and most importantly, they can be readily used for trace concentration gas detection integrated in a large scale. In the meanwhile, the response and recovery times are not influenced by the FET circuit, which are seconds as the original ones as shown in Figs. 3-5. Therefore, this signal amplification circuit is promising for the fast and effective detection of environmental VOCs and people breath compositions.

TABLE I
COMPARISON OF THE TYPICAL TOLUENE, ACETONE AND ETHANOL GAS SENSORS

Sensor type	Conc. (ppm)	Response (Ra/Rg)	Reference
Toluene			
TGS2602	1	~ 3	Manual
	1	~ 7 with FET	This work
rGO/Co_3O_4	5	11.3	[27]
Pt-SnO_2/ZnO	0.1	279	[22]
α-Fe_2O_3/NiO	5	8.8	[9]
Acetone			
MP502	10	~ 4	Manual
	10	~ 17 with FET	This work
In_2O_3/Au	10	~ 6	[7]
W-NiO	8	~ 13.5	[34]
C-WO_3	5	~ 8	[8]
Ethanol			
MQ3	50	~ 6	Manual
	50	~ 35 with FET	This work
ZnO nanorods	50	~ 30	[35]
Al-doped NiO	50	~ 10	[36]
Pt-SnO_2	5	~ 1400	[37]
In_2O_3/Au	5	~ 12	[7]

C. Mechanism

We study the mechanism how the FET K544 amplified the apparent response of toluene sensors (Figaro TGS2602, Japan). From the FET viewpoint in Fig. 1a, the V_{OUT} can be

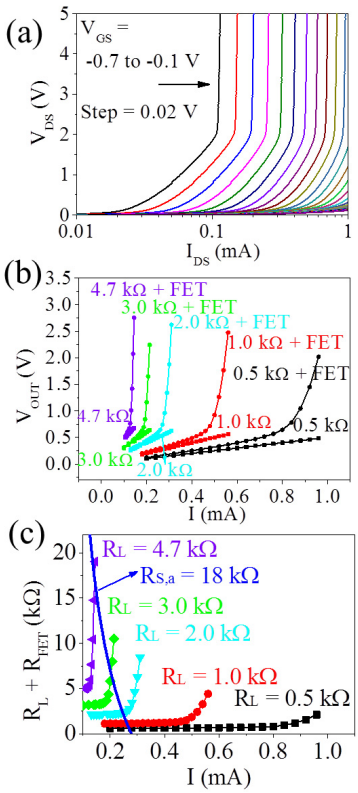

Fig. 6. K544 FET characteristics for the amplification mechanism. (a) V_{DS}-I_{DS} curves of FET K544, V_{GS} changes from −0.7 V to −0.1 V (step is 0.02 V). (b) Output voltage versus current cures of two kinds of electric circuits. Lines are data of the conventional electric circuit without FET while curves are date of the amplification circuit with FET. (c) (R_L+ R_{FET}) resistance calculation using data in b.

calculated by the gate voltage and drain voltage as (5):

$$V_{OUT} = -V_{GS} + V_{DS}. \tag{5}$$

Therefore, the V_{OUT} can be estimated by the voltage characteristics of the FET. Then the I_{DS}− V_{DS} curves of FET K544 at different V_{GS} are measured as shown in Fig. 6a. In air, the current can be estimated by the bias voltage (5 V) and the resistance of the circuit ($R_{S,a}$ ∼ 18.0 kΩ, and R_L ∼ 2.0 kΩ), which is about 0.25 mA. Then the V_{GS} of the FET is -0.25 mA × 2.0 kΩ = -0.5 V. The V_{DS} can thus be estimated from Fig. 6a at the point of I_{DS} = 0.25 mA and V_{GS} = −0.5 V to be V_{DS} ∼ 0.06 V. Therefore, V_{OUT} in air is 0.56 V. Then the V_{OUT} – I curves can be drawn by varying the current and R_L as shown in Fig. 6b. As a comparison, the V_{OUT} – I curves of the R_L without FET are also drawn, where one can clearly see a sharp V_{OUT} increase, especially with the large R_L of 4.7 kΩ. However, the MF is the highest using R_L = 2.0 kΩ in Fig. 3, because MF should be calculated by (R_L+ $R_{FET,g}$) / (R_L+ $R_{FET,a}$) as discussed above. Then (R_L + R_{FET}) is calculated by V_{OUT} / I using the data in Fig. 6b, which is shown in Fig. 6c. The value of (R_L+ $R_{FET,a}$) can be estimated by the intersection point with the curve (R_L+ R_{FET}) = 5/I − $R_{S,a}$, as shown in Figure 6c with typical $R_{S,a}$ of 18 kΩ. On the other side, the FET could reach the saturation current seen from Fig. 6a, as the increased current will enhance V_{GS} (V_{GS} = I × R_L) which on the contrary will depress current as shown in Fig. 2c. The (R_L + R_{FET}) - I curves of the amplification circuit with FET are fitted to calculate the R_L+ $R_{FET,\,g}$ as shown in Fig. S2. According to fitted formulas, we could compute the R_L+ $R_{FET,g}$ value when a maximum current value is put in the corresponding formula as shown in Table II. It should be noted in Fig. 6c that the R_L+ $R_{FET,a}$ value (about 2.3 kΩ) is similar to that without FET (2.0 kΩ). This is the main reason why this FET amplification circuit will not amplify the noise because the baseline in air is similar to the case without FET amplifier as shown in Figs. 2-5. Then MF can be easily estimated by the resistance change, as shown in Table II. It is noticed that the estimated theoretical MF is in good consistence with those observed. Therefore, the FET amplification circuit can now work well for the MOX sensors from both mechanism and technological aspects, with the largest MF of 5-6 for all the three sensors to different gases in Figs. 3-5. It should also be noted that the load resistance can well selected from Fig. 6c to get a maximum MF. For example, if R_S is about 20 kΩ, the load resistance R_L should be about 2 kΩ to obtain a low R_L+ $R_{FET,a}$, and thus a high MF. Otherwise, if R_L is selected as 4.7 kΩ, R_L+ $R_{FET,a}$ is high while R_L+ $R_{FET,g}$ is the same, meaning low MF as shown in Fig. 3.

TABLE II

THEORETICAL AND ACTUAL MAGNIFICATION FACTORS (MF) OF K544 FET WITH DIFFERENT LOAD RESISTANCES R_L TO 20 PPM TOLUENE

R_L kΩ	$R_L + R_{FET,a}$ [1] kΩ	$R_L + R_{FET,g}$ [2] kΩ	Theoretical MF	Measured MF
0.5	0.62	3.08	5.0	4.9
1.0	1.14	5.39	4.7	4.0
2.0	2.30	12.86	5.6	5.1
3.0	3.99	16.12	4.0	4.2
4.7	17.06	28.98	1.7	1.4

(1) $R_L + R_{FET,a}$ is calculated by the intersection point similar to Fig. 6c.
(2) $R_L + R_{FET,g}$ is calculated by the fitted curves in Fig. S2.

From the above experimental results and theoretical analyses, the advantages of the FET amplification circuits can be summarized and compared with conventional operational amplifier circuits. Firstly, this FET circuit is simple using only one transistor while several operational amplifiers and resistors/capacitors are needed traditionally. Therefore, the volume and power consumption would be far lower for FET amplifiers. Second, the FET amplifier enhances only signal but not baseline or noise, while careful design and parameter optimization should be taken for operational amplifiers to adjust offset and filter noise.

V. CONCLUSION

A signal amplification circuit using field effect transistor (FET) is designed and integrated for metal oxide gas sensors for the detection of gases at low concentrations. For the proof of concept, Japanese Figaro TGS2602, Chinese Hanwei MP502 and MQ3 sensors are adopted to detect toluene, acetone and ethanol at low concentration of sub-ppm and ppm levels. The FET is optimized to be K544 with ideal subthreshold slop, and the load resistance is optimized to be 2.0 kΩ for toluene sensor, 14.7 kΩ for acetone sensor and 1.0 kΩ for ethanol sensor. The amplification mechanism is

found to be the resistance change of the FET by applying the gate voltage, and the theoretical magnification is estimated to be in good agreement with that measured. This signal amplification circuit shows the advantage in low concentration gas detection in environment and health, which can be readily integrated using the commercial electronics. And this circuit design is also promising in other kind of sensors to extend the detection limit to low concentrations.

REFERENCES

[1] N. Yamazoe, "Toward innovations of gas sensor technology," *Sens. Actuators B, Chem.*, vol. 108, nos. 1–2, pp. 2–14, Jul. 2005.

[2] M. Tiemann, "Porous metal oxides as gas sensors," *Chem.-Eur. J.*, vol. 13, no. 30, pp. 8376–8388, 2007.

[3] K. Potje-Kamloth, "Semiconductor junction gas sensors," *Chem. Rev.*, vol. 108, no. 2, pp. 367–399, Feb. 2008.

[4] N. Barsan, D. Koziej, and U. Weimar, "Metal oxide-based gas sensor research: How to?" *Sens. Actuators B, Chem.*, vol. 121, no. 1, pp. 18–35, Jan. 2007.

[5] X. Wang *et al.*, "Room temperature resistive volatile organic compound sensing materials based on a hybrid structure of vertically aligned carbon nanotubes and conformal oCVD/iCVD polymer coatings," *ACS Sensors*, vol. 1, no. 4, pp. 374–383, 2016.

[6] A. T. Güntner, V. Koren, K. Chikkadi, M. Righettoni, and S. E. Pratsinis, "E-nose sensing of low-ppb formaldehyde in gas mixtures at high relative humidity for breath screening of lung cancer?" *ACS Sensors*, vol. 1, no. 5, pp. 528–535, 2016.

[7] R. Q. Xing *et al.*, "Preparation and gas sensing properties of In_2O_3/Au nanorods for detection of volatile organic compounds in exhaled breath," *Sci. Rep.*, vol. 5, Jun. 2015, Art. no. 10717.

[8] T. Xiao *et al.*, "Highly sensitive and selective acetone sensor based on C-doped WO_3 for potential diagnosis of diabetes mellitus," *Sens. Actuators B, Chem.*, vol. 199, pp. 210–219, Aug. 2014.

[9] C. Wang *et al.*, "Design of α-Fe_2O_3 nanorods functionalized tubular NiO nanostructure for discriminating toluene molecules," *Sci. Rep.*, vol. 6, May 2016, Art. no. 26432.

[10] Y. Guan *et al.*, "Hydrothermal preparation and gas sensing properties of Zn-doped SnO_2 hierarchical architectures," *Sens. Actuators B, Chem.*, vol. 191, pp. 45–52, Feb. 2014.

[11] N. Han, L. Chai, Q. Wang, Y. Tian, P. Deng, and Y. Chen, "Evaluating the doping effect of Fe, Ti and Sn on gas sensing property of ZnO," *Sens. Actuators B, Chem.*, vol. 147, no. 2, pp. 525–530, Jun. 2010.

[12] N. Han, X. Wu, D. Zhang, G. Shen, H. Liu, and Y. Chen, "CdO activated Sn-doped ZnO for highly sensitive, selective and stable formaldehyde sensor," *Sens. Actuators B, Chem.*, vol. 152, no. 2, pp. 324–329, Mar. 2011.

[13] A. Kolmakov, D. O. Klenov, Y. Lilach, S. Stemmer, and M. Moskovits, "Enhanced gas sensing by individual SnO_2 nanowires and nanobelts functionalized with Pd catalyst particles," *Nano Lett.*, vol. 5, no. 4, pp. 667–673, Apr. 2005.

[14] Y. J. Kwon, H. G. Na, S. Y. Kang, S.-W. Choi, S. S. Kim, and H. W. Kim, "Selective detection of low concentration toluene gas using Pt-decorated carbon nanotubes sensors," *Sens. Actuators B, Chem.*, vol. 227, pp. 157–168, May 2016.

[15] X. Zou *et al.*, "Rational design of sub-parts per million specific gas sensors array based on metal nanoparticles decorated nanowire enhancement-mode transistors," *Nano Lett.*, vol. 13, no. 7, pp. 3287–3292, Jul. 2013.

[16] J. H. He, C. H. Ho, and C. Y. Chen, "Polymer functionalized ZnO nanobelts as oxygen sensors with a significant response enhancement," *Nanotechnology*, vol. 20, no. 6, p. 065503, Feb. 2009.

[17] J. Kong, M. G. Chapline, and H. Dai, "Functionalized carbon nanotubes for molecular hydrogen sensors," *Adv. Mater.*, vol. 13, no. 18, pp. 1384–1386, Sep. 2001.

[18] D. Ju, H. Xu, Z. Qiu, J. Guo, J. Zhang, and B. Cao, "Highly sensitive and selective triethylamine-sensing properties of nanosheets directly grown on ceramic tube by forming NiO/ZnO PN heterojunction," *Sens. Actuators B, Chem.*, vol. 200, pp. 288–296, Sep. 2014.

[19] S.-J. Kim, C. W. Na, I.-S. Hwang, and J.-H. Lee, "One-pot hydrothermal synthesis of CuO–ZnO composite hollow spheres for selective H_2S detection," *Sens. Actuators B, Chem.*, vol. 168, pp. 83–89, Jun. 2012.

[20] X. Xue, L. Xing, Y. Chen, S. Shi, Y. Wang, and T. Wang, "Synthesis and H_2S sensing properties of CuO-SnO_2 core/shell PN-junction nanorods," *J. Phys. Chem. C*, vol. 112, no. 32, pp. 12157–12160, Aug. 2008.

[21] W. Zang, Y. Nie, D. Zhu, P. Deng, L. Xing, and X. Xue, "Core–shell In_2O_3/ZnO nanoarray nanogenerator as a self-powered active gas sensor with high H_2S sensitivity and selectivity at room temperature," *J. Phys. Chem. C*, vol. 118, no. 17, pp. 9209–9216, May 2014.

[22] J.-H. Kim and S.-S. Kim, "Realization of ppb-scale toluene-sensing abilities with Pt-functionalized SnO_2–ZnO core–shell nanowires," *ACS Appl. Mater. Interfaces*, vol. 7, no. 31, pp. 17199–17208, Aug. 2015.

[23] A. Katoch, S.-W. Choi, G.-J. Sun, and S. S. Kim, "An approach to detecting a reducing gas by radial modulation of electron-depleted shells in core–shell nanofibers," *J. Mater. Chem. A*, vol. 1, no. 43, pp. 13588–13596, 2013.

[24] X. Pan, X. Liu, A. Bermak, and Z. Fan, "Self-gating effect induced large performance improvement of ZnO nanocomb gas sensors," *ACS Nano*, vol. 7, no. 10, pp. 9318–9324, Oct. 2013.

[25] N. Singh, R. K. Gupta, and P. S. Lee, "Gold-nanoparticle-functionalized In_2O_3 nanowires as CO gas sensors with a significant enhancement in response," *ACS Appl. Mater. Interfaces*, vol. 3, no. 7, pp. 2246–2252, Jul. 2011.

[26] Y. Bing *et al.*, "Multistep synthesis of non-spherical SnO_2@SnO_2 yolk-shell cuboctahedra with nanoparticle-assembled porous structure for toluene detection," *Sens. Actuators B, Chem.*, vol. 231, pp. 365–375, Aug. 2016.

[27] S. Bai *et al.*, "Preparation of reduced graphene oxide/Co_3O_4 composites and sensing performance to toluene at low temperature," *RSC Adv.*, vol. 6, no. 65, pp. 60109–60116, 2016.

[28] C. Falconi *et al.*, "Electronic interfaces," *Sens. Actuators B, Chem.*, vol. 121, no. 1, pp. 295–329, 2007.

[29] A. De Marcellis, G. Ferri, and P. Mantenuto, "Resistive sensor interfacing," in *Giant Magnetoresistance (GMR) Sensors*, vol. 6, 2013, pp. 71–102.

[30] J. W. Gardner, P. K. Guha, F. Udrea, and J. A. Covington, "CMOS interfacing for integrated gas sensors: A review," *IEEE Sensors J.*, vol. 10, no. 12, pp. 1833–1848, Dec. 2010.

[31] X. F. Liang and L. H. Liu, "Design on the amplifier circuit of metal-oxide semiconductor gas-sensitive sensor," *Appl. Mech. Mater.*, vols. 220–223, pp. 1939–1942, Nov. 2012.

[32] N. Qin, X. Wang, Q. Xiang, and J. Xu, "A biomimetic nest-like ZnO: Controllable synthesis and enhanced ethanol response," *Sens. Actuators B, Chem.*, vol. 191, pp. 770–778, Feb. 2014.

[33] X. Zhou *et al.*, "Nanosheet-assembled $ZnFe_2O_4$ hollow microspheres for high-sensitive acetone sensor," *ACS Appl. Mater. Interfaces*, vol. 7, no. 28, pp. 15414–15421, Jul. 2015.

[34] C. Wang *et al.*, "Ultrasensitive and low detection limit of acetone gas sensor based on W-doped NiO hierarchical nanostructure," *Sens. Actuators B, Chem.*, vol. 220, pp. 59–67, Dec. 2015.

[35] S. Tian, F. Yang, D. Zeng, and C. Xie, "Solution-processed gas sensors based on ZnO nanorods array with an exposed (0001) facet for enhanced gas-sensing properties," *J. Phys. Chem. C*, vol. 116, no. 19, pp. 10586–10591, May 2012.

[36] C. Wang *et al.*, "Design of superior ethanol gas sensor based on Al-doped NiO nanorod-flowers," *ACS Sensors*, vol. 1, no. 2, pp. 131–136, 2016.

[37] B.-Y. Kim *et al.*, "Extremely sensitive ethanol sensor using Pt-doped SnO_2 hollow nanospheres prepared by Kirkendall diffusion," *Sens. Actuators B, Chem.*, vol. 234, pp. 353–360, Oct. 2016.

Xinyuan Zhou received the B.S. degree in materials chemistry from the Taiyuan University of Technology in 2010. He is currently pursuing the Ph.D. degree in materials engineering with the Institute of Process Engineering, Chinese Academy of Sciences.

Ying Wang received the bachelor's degree in optics from Beijing Jiaotong University, in 2010, and the Ph.D. degree in physical electronics from the College of Electronics, Peking University.

Jinxiao Wang received the bachelor's degree in chemical engineering and technology from the Xi'an University of Architecture and Technology in 2014, where he is currently pursuing the M.S. degree.

Zheng Xie received the bachelor's degree in chemical engineering and technology from the Tianjin University of Science and Technology in 2014. He is currently pursuing the M.S. degree in chemical engineering and technology with the Beijing University of Chemical Technology.

Xiaofeng Wu received the Ph.D. degree from the Institute of Process Engineering, Chinese Academyof Sciences, in 2007. He joined the Institute of Process Engineering in 2009, and is currently a Professor with the Institute of Process Engineering. His research interests are preparation of nanostructural inorganic materials (metal@oxide semiconductor core-shell and hollow particles) and their application in sensors, photocatalysis, thermal insulator, and energy storage.

Ning Han received the Ph.D. degree in chemical engineering from the Institute of Process Engineering, CAS, in 2010. He was a Post-Doctoral Fellow with the Department of Physics and Materials Science, City University of Hong Kong, from 2010 to 2014, and has been a Professor with Institute of Process Engineering, Chinese Academy of Sciences via One Hundred Talents Plan since 2014. He works on investigations of preparation, structure, and property of semiconductors, and has developed highly sensitive and selective gas sensing materials. He has authored over 60 articles.

Yunfa Chen received the Ph.D. degree in material science from Université Louis Pasteur Strasbourg, France, in 1993. He is currently a Professor with the Graduate University of Chinese Academy of Sciences, and a Research Professor and Vice Director of the Institute of Process Engineering, Chinese Academy of Sciences. His current research interests are preparation and assembly of nanoparticles, functional materials, organic-inorganic composite materials and layered materials, and industrial application of nanomaterials.